Available online at www.sciencedirect.com
SCIENCE DIRECT®
Journal of Sound and Vibration 292 (2006) 504–518
JOURNAL OF SOUND AND VIBRATION
www.elsevier.com/locate/jsvi

Analytical solution of multimodal acoustic propagation in circular ducts with laminar mean flow profile

R. Boucheron, H. Bailliet, J.-C. Valiere*

Laboratoire d'Études Aérodynamiques, C.N.R.S. UMR 6609, Université de Poitiers, 40, Avenue du Recteur Pineau, Bât K. 86022 Poitiers Cedex, France

Received 4 December 2003; received in revised form 6 June 2005; accepted 9 August 2005
Available online 2 November 2005

Abstract

In this paper, an analytical solution for the propagation of sound in circular ducts in the presence of Poiseuille mean flow is derived. This solution uses Kummer's functions and it generalizes the results found by Gogate and Munjal. Links between this solution and already-known solutions for more specific cases (no mean flow, uniform flow) are made. Results for calculation of the propagation constant and pressure profiles are presented and compared with the literature. The effect of shear on multimodal acoustic propagation, including modes of higher radial order is discussed.

1. Introduction

The acoustic propagation in ducts having parallel mean shear flow is one of the research topics with wide engineering applications. When a pipe contains a non-uniform flow, the convected wave equation which governs acoustic propagation does not generally allow any simple analytical solution as in the no flow and uniform flow cases [1,2]. Therefore, analysis of wave propagation in ducts with shear mean flow has been done, in most cases, numerically [3–5]. But the analytic modal description of the sound field which we are concerned with in this study can provide more physical insight into global behaviour than a numerical solution.

Pridmore-Brown [6] first established the modal equation governing transverse mode propagation in ducts containing parallel shear flow. Mungur and Plumbee [7] derived the convected wave equation for acoustic wave propagation in a fully developed duct flow, which corresponds to a turbulent flow confined to the axial direction. An analytical solution for sound propagation in the presence of Poiseuille mean flow was derived by Gogate and Munjal [8,9] in the particular case of axi-symmetric modes. Pagneux and Froelich [10] studied both theoretically (by means of a perturbation expansion at a low Mach number of the Pridmore-Brown equation, like Peube and Jallet [11]) and experimentally (by means of pressure measurements) the multimodal acoustic propagation in low Mach number shear flow ducts.

*Corresponding author. Tel.: +33 5 49 45 33 59; fax: +33 5 49 45 36 63.
E-mail address: jean-christophe.valiere@lea.univ-poitiers.fr (J.-C. Valiere).
URL: http://www-lea.univ-poitiers.fr.

0022-460X/$ - see front matter © 2005 Elsevier Ltd. All rights reserved.
doi:10.1016/j.jsv.2005.08.017

Numerical studies on propagation of sound in a duct in the presence of a mean flow and/or a temperature gradient were conducted in the last few years [12–16]. Agarwal and Bull [12] solved the convected wave equation for acoustic wave propagation in a fully developed duct flow numerically, for both upstream and downstream wave propagation. They determined the cut-off frequency and the propagation constant of any specified acoustic mode as well as the radial distribution of the acoustic pressure and velocity for this configuration. Also, many studies in the field of flow duct acoustic propagation are concerned with the question of attenuation in lined ducts such as encountered in silencers and mufflers (e.g. Ref. [17]). Concerning this problem, Kakoty and Roy [18] recently presented a general formulation for the analysis of sound in a uniform flow duct lined with bulk-reacting sound-absorbing material. They used a Newton–Raphson scheme whereas most of the previous works on this subject were based on the finite-element formulation which does not include all types of modes or does not include mean flow effects.

In this paper, we are concerned with the analytical study of multimodal acoustic propagation in circular hard wall ducts in the case of a low Mach number and low Reynolds number mean flow (laminar subsonic mean flow). The available solution for such a problem, proposed by Gogate and Munjal [8,9], which is valid for axi-symmetric modes only, is extended to other modes of propagation. In Section 2, the wave equation is derived and the already-known Pridmore-Brown equation is established. A solution of this equation is then obtained in the case of a laminar mean flow profile. In Section 3, this solution is linked with solutions of sound propagation in more specific cases. Section 4 outlines the eigenmodes found for a hard wall duct. In Section 5, results of the calculation of the propagation constant and acoustic pressure profiles are compared with previous results of numerical calculation and the effect of shear flow is discussed.

2. Governing equations

We consider sound propagation in a circular duct with a laminar mean velocity profile $u_0(r)$ (see Fig. 1) that is independent of x. In such a configuration, the Pridmore-Brown equation that governs wave propagation is obtained from the mass continuity and momentum equations. If the effect of viscosity is neglected and if it is assumed that the thermal conductivity of the fluid is negligible so that the entropy perturbations of the system can be taken to be zero, these equations, written to the first order in cylindrical coordinates (x, r, θ), are (e.g. Ref. [8])

$$\frac{1}{c_0^2}\frac{Dp}{Dt} + \rho_0\left[\frac{\partial u}{\partial x} + \frac{1}{r}\frac{\partial}{\partial r}(rv) + \frac{1}{r}\frac{\partial w}{\partial \theta}\right] = 0 \tag{1}$$

for the continuity equation, and

$$\rho_0\frac{Du}{Dt} + \rho_0 v\frac{\partial u_0}{\partial r} = -\frac{\partial p}{\partial x}, \tag{2}$$

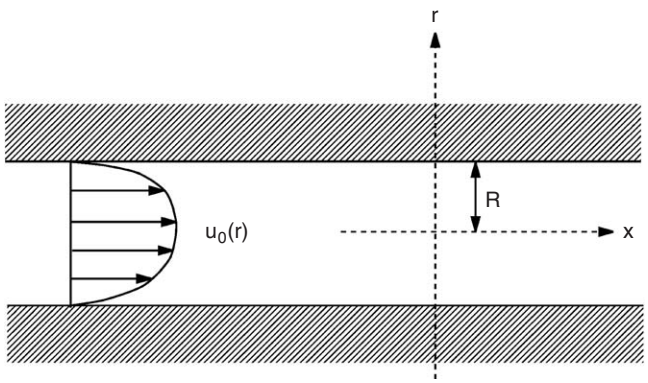

Fig. 1. Configuration of the problem.

$$\rho_0 \frac{Dv}{Dt} = -\frac{\partial p}{\partial r}, \tag{3}$$

$$\rho_0 \frac{Dw}{Dt} = -\frac{1}{r}\frac{\partial p}{\partial \theta} \tag{4}$$

for the x, r and θ components of the momentum equations. Here the x, r and θ components of the fluid velocity are

$$\mathbf{u} = \begin{pmatrix} u_0(r) + u(x, r, \theta, t) \\ v(x, r, \theta, t) \\ w(x, r, \theta, t) \end{pmatrix},$$

c_0 is the speed of sound, ρ_0 the mean density, p the acoustic pressure. The subscript 0 refers to zero-order, that are constant quantities. D/Dt is the material derivative, expressed as

$$\frac{D}{Dt} = \frac{\partial}{\partial t} + u_0 \frac{\partial}{\partial x}.$$

Combining the divergence of momentum equation with the material derivative of continuity equation leads to the following equation [10,12,19]:

$$\nabla^2 p - \frac{1}{c_0^2}\frac{D^2 p}{Dt^2} + 2\rho_0 \frac{\partial u_0}{\partial r}\frac{\partial v}{\partial x} = 0 \tag{5}$$

with ∇^2 the Laplacian operator. This is the classic equation for sound propagation together with an additional term (the third one) that represents the effect of shear flow. Developing each term and introducing the Mach number, defined as $\mathscr{M}(r) = u_0(r)/c_0$, yields

$$\nabla^2 p - \frac{1}{c_0^2}\frac{\partial^2 p}{\partial t^2} - 2\frac{\mathscr{M}}{c_0}\frac{\partial^2 p}{\partial x \partial t} - \mathscr{M}^2 \frac{\partial^2 p}{\partial x^2} + 2\rho_0 c_0 \frac{\partial \mathscr{M}}{\partial r}\frac{\partial v}{\partial x} = 0. \tag{6}$$

We consider a harmonic wave propagating either in the direction of flow (downstream propagation) or in the opposite direction (upstream propagation). Acoustic pressure and velocity are proportional to $\exp[\mathrm{i}(\gamma x - \omega t + m\theta)]$ (or $\exp[\mathrm{i}(-\gamma x - \omega t + m\theta)]$) in the case of downstream propagation (respectively, upstream propagation), where m is the circumferential mode order and γ is the propagation constant (which can be complex). When introducing the non-dimensional propagation constant defined as $\Gamma = c_0\gamma/\omega$, the material derivative becomes

$$\frac{D}{Dt} = \frac{\partial}{\partial t} + u_0 \frac{\partial}{\partial x} = -\mathrm{i}\omega(1 \mp \mathscr{M}\Gamma),$$

where here and henceforth, upper/lower signs are to be taken for the downstream/upstream propagation, respectively. Using the momentum equation over r, Eq. (3), it follows that [7]

$$2\rho_0 c_0 \frac{\partial v}{\partial x} = \frac{\pm 2\Gamma}{1 \mp \mathscr{M}\Gamma}\frac{\partial p}{\partial r}, \tag{7}$$

which, replaced in Eq. (6), gives

$$\nabla^2 p - \frac{1}{c_0^2}\frac{\partial^2 p}{\partial t^2} - 2\frac{\mathscr{M}}{c_0}\frac{\partial^2 p}{\partial x \partial t} - \mathscr{M}^2 \frac{\partial^2 p}{\partial x^2} + \frac{\pm 2\Gamma}{1 \mp \mathscr{M}\Gamma}\frac{\partial \mathscr{M}}{\partial r}\frac{\partial p}{\partial r} = 0. \tag{8}$$

The pressure can be written as $p = BP(r)\exp[\mathrm{i}(\pm\gamma x - \omega t + m\theta)]$, where B is a constant that depends on the initial conditions and $P(r)$ is the acoustic pressure profile. Using this expression, introducing non-dimensional parameters $\xi = r/R$, $\Omega = \omega R/c_0$ and using $\mathscr{M}(\xi) = u_0(\xi)/c_0$ leads to the Pridmore-Brown equation [6]

$$\frac{\partial^2 P}{\partial \xi^2} + \left(\frac{1}{\xi} + \frac{\pm 2\Gamma}{1 \mp \mathscr{M}\Gamma}\frac{\partial \mathscr{M}}{\partial \xi}\right)\frac{\partial P}{\partial \xi} + \Omega^2\left((1 \mp \mathscr{M}\Gamma)^2 - \Gamma^2 - \frac{m^2}{\Omega^2\xi^2}\right)P = 0. \tag{9}$$

For a typical laminar mean flow, that is for a low Reynolds number, the profile of the mean velocity over the duct section can be expressed as $\mathscr{M}(\xi) = \mathscr{M}_0(1-\xi^2)$ with $\mathscr{M}_0$ defined as the centreline Mach number. Introducing this equation into Eq. (9) leads to the wave equation for laminar mean flow

$$\frac{\partial^2 P}{\partial \xi^2} + \left(\frac{1}{\xi} - \frac{\pm 4\mathscr{M}_0 \Gamma \xi}{1 \mp \Gamma \mathscr{M}_0(1-\xi^2)}\right)\frac{\partial P}{\partial \xi} + \Omega^2\left((1 \mp \Gamma \mathscr{M}_0(1-\xi^2))^2 - \Gamma^2 - \frac{m^2}{\Omega^2 \xi^2}\right)P = 0. \tag{10}$$

This equation, together with the hard-walled duct boundary conditions, consists in the problem to be solved. It cannot be solved analytically. However, we show in the following that it allows an analytical solution in the case of a low Mach number.

3. Low Mach number solution and its link with already-known solutions

Using $|\mathscr{M}_0\Gamma|^2 \ll 1$, the coefficients of the differential equation (10) can be developed as

$$\frac{1}{\xi} - \frac{\pm 4\mathscr{M}_0\Gamma\xi}{1 \mp \mathscr{M}_0\Gamma(1-\xi^2)} \approx \frac{1 \mp 4\mathscr{M}_0\Gamma\xi^2}{\xi},$$

$$(1 \mp \mathscr{M}_0\Gamma(1-\xi^2))^2 - \Gamma^2 \approx (1 \mp 2\mathscr{M}_0\Gamma - \Gamma^2) \pm 2\mathscr{M}_0\Gamma\xi^2, \tag{11}$$

which leads to the differential equation

$$\frac{\partial^2 P}{\partial \xi^2} + \left(\frac{1-a\xi^2}{\xi}\right)\frac{\partial P}{\partial \xi} + \left(b + c\xi^2 - \frac{m^2}{\xi^2}\right)P = 0 \tag{12}$$

with $a = \pm 4\mathscr{M}_0\Gamma$, $b = \Omega^2(1 \mp 2\mathscr{M}_0\Gamma - \Gamma^2)$ and $c = \pm 2\mathscr{M}_0\Gamma\Omega^2$.

Then, introducing $\alpha = \sqrt{a^2 - 4c}$, it appears that this differential equation allows an analytical solution (see appendix for more details)

$$P(\xi) = \left(\frac{\alpha}{2}\right)^{(m+1)/2} e^{([(a-\alpha)/4]\xi^2)}\xi^m \mathscr{K}\left(\frac{(m+1)\alpha - (a+b)}{2\alpha}, m+1, \frac{\alpha}{2}\xi^2\right), \tag{13}$$

where $\mathscr{K}$ is the Kummer's M-function. This is the general analytical solution for sound propagation in a circular duct with laminar mean flow that is valid for a low Mach number.

Notice that this solution is available for low Mach number, according to $|\mathscr{M}_0\Gamma|^2 \ll 1$. This restriction is frequency independent, that is the solution of acoustic pressure profile is available for all frequencies. Typically, values of Γ are of order of magnitude of 1. Therefore, the solution is available for Mach number less than 0.3.

In the following, links between this solution and already-known solutions for more specific cases are outlined.

3.1. Link with Gogate and Munjal solution

Gogate and Munjal [8] derived a solution for sound propagation in circular ducts in the specific case of axi-symmetric modes ($m = 0$). The solution given by Eq. (13) is a generalization of this solution. Indeed, axi-symmetric modes are given by setting $m = 0$ in Eq. (13), leading to the following expression for the pressure amplitude:

$$P(\xi) = \left(\frac{\alpha}{2}\right)^{1/2} e^{((a-\alpha)/4)} \mathscr{K}\left(\frac{\alpha - a - b}{2\alpha}, 1, \frac{\alpha}{2}\xi^2\right),$$

which is exactly the solution derived by Gogate [8] (see [8, Eq. (29)]).

3.2. Link with the no flow solution

In the case of no mean flow (Mach number equals zero), the Pridmore-Brown equation (Eq. (9)) can be simplified and gives the Bessel equation

$$\frac{\partial^2 P}{\partial \xi^2} + \frac{1}{\xi}\frac{\partial P}{\partial \xi} + \left(\Omega^2 - (\Omega\Gamma)^2 - \frac{m^2}{\xi^2}\right)P = 0.$$

Solutions of this differential equation are, for a physical problem, the Bessel functions of the first kind $J_m(x)$. The pressure can then be expressed as a combination of the eigenmodes as [1,2]

$$p(x,\xi,\theta,t) = \sum_{m=-\infty}^{\infty}\sum_{n=0}^{\infty} C_{m,n} J_m(\kappa_{m,n}\xi) e^{i(\omega t \mp \gamma x + m\theta)} \tag{14}$$

with

$$J'_m(\kappa_{m,n}) = 0 \quad \text{and} \quad \kappa^2_{m,n} = \Omega^2(1-\Gamma^2), \tag{15}$$

where the coefficients $C_{m,n}$ depend on the initial conditions of the physical problem. Here, n is the radial mode order, $\kappa_{m,n}$ is the non-dimensional radial wavenumber. Nodal representation of these eigenmodes is shown in Fig. 2.

The solution (14) can be compared with the limiting case of solution (13) that corresponds to $\mathscr{M} \longrightarrow 0$, which implies $a \longrightarrow 0$, $c \longrightarrow 0$ and $\alpha \longrightarrow 0$. Using the following Kummer function limit property (see (13.5.13) of Ref. [20]):

$$\lim_{\rho\to\infty} \mathscr{K}(\rho,\mu,\beta) = \Gamma(\mu) e^{(1/2)\beta} (\tfrac{1}{2}\mu\beta - \rho\beta)^{((1/2)-(1/2)\mu)} J_{\mu-1}\left(\sqrt{2\mu\beta - 4\rho\beta}\right),$$

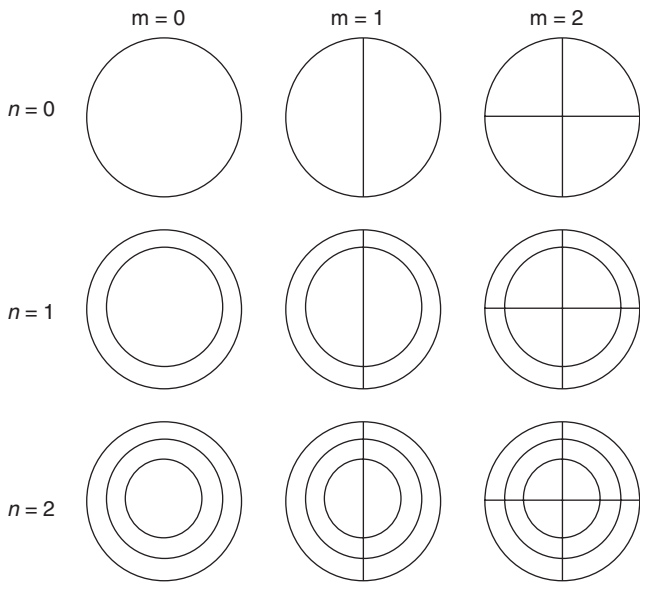

Fig. 2. Nodal representation of the mode profiles in the (m,n) coordinate system.

the no flow pressure profile (13) can be written as

$$P(\xi) = \lim_{a,c,\alpha\to 0}\left[\left(\frac{\alpha}{2}\right)^{(m+1)/2} e^{([(a-\alpha)/4]\,\xi^2)}\,\xi^m \Gamma(m+1) e^{((\alpha/4)\xi^2)} \times\left(\frac{(m+1)\alpha\xi^2}{4} - \frac{(m+1)\alpha-(a+b)}{4}\,\xi^2\right)^{-m/2} J_m\left(\sqrt{(a+b)\xi^2}\right)\right]$$
$$\propto J_m\left(\sqrt{b}\xi\right)$$

with J_m the mth Bessel function of the first kind. Since $b = \Omega^2(1-\Gamma^2)$ this solution is in fact the well-known analytic solution for modal propagation of sound in a circular duct.

In the case where the mean flow is supposed to be uniform over the duct section, that is in the case of a constant Mach number over the cross-section, the governing equations do not yield to Pridmore-Brown solution but to a Bessel equation (e.g. Ref. [1])

$$\frac{\partial^2 P}{\partial \xi^2} + \frac{1}{\xi}\frac{\partial P}{\partial \xi} + \left((\Omega - \mathscr{M}_0\Omega\Gamma)^2 - (\Omega\Gamma)^2 - \frac{m^2}{\xi^2}\right)P = 0.$$

The solution for the pressure profile is the same as in the case of no mean flow except that the eigenfrequencies are shifted by the Mach number, according to

$$\kappa_{m,n}^2 = \Omega^2[(1-\mathscr{M}_0\Gamma)^2 - \Gamma^2]. \tag{16}$$

At this stage it is possible to determine the eigenmodes and the corresponding eigenfrequencies in the cases of both the no flow and uniform flow configurations as well as in the case of laminar shear flow. This is done in the next section.

4. Eigenmodes of the solution

4.1. Dispersion equation

For each eigenmode (m,n), the propagation constant Γ can be determined by writing the boundary conditions for a given flow, that is for a given Mach number and frequency excitation (Ω). This is done by means of the dispersion equation: Eq. (15) in the case of no flow and Eq. (16) in the case of uniform flow. In the case of laminar shear flow, it is first necessary to establish the dispersion equation. In any case, roots of the dispersion equation can be real or complex. Real roots correspond to the propagative eigenmodes, whereas complex roots correspond to evanescent eigenmodes. The case $\Gamma = 0$ represents the cut-off frequency of the mode. If the working frequency is lower than the cut-off frequency then the wave is evanescent, whereas if it is larger then the wave propagates.

As stated above, in the case of a laminar shear flow, the dispersion equation should be determined. This is done using the hard-wall condition, which can be written as (using Eq. (2))

$$[v(\xi)]_{\xi=1} = \frac{\mathrm{i}}{\omega\rho_0 R}\left[\frac{\partial P(\xi)}{\partial \xi}\right]_{\xi=1} = 0.$$

Using Eq. (13) yields an expression of the transverse velocity at the wall as

$$[v(\xi)]_{\xi=1} = \left[\mathrm{i}\,\frac{\left(\frac{\alpha}{2}\right)^{(m+1)/2}\,\xi^m e^{([(a-\alpha)/4]\xi^2)}}{\omega\rho_0 R} \times\left(\alpha\xi\mathscr{K}'\left(A, m+1, \frac{\alpha}{2}\,\xi^2\right) + \left(\frac{2(a-\alpha)\xi}{4} + \frac{m}{\xi}\right)\mathscr{K}\left(A, m+1, \frac{\alpha}{2}\,\xi^2\right)\right)\right]_{\xi=1} \tag{17}$$

with

$$A = \frac{(m+1)\alpha - (a+b)}{2\alpha}.$$

It follows that the propagation constants are found by solving the following dispersion equation in Γ:

$$F(\Gamma) = \frac{\alpha A}{m+1}\,\mathscr{K}\left(A+1, m+2, \frac{\alpha}{2}\right) + \frac{a-\alpha+2m}{2}\,\mathscr{K}\left(A, m+1, \frac{\alpha}{2}\right) = 0, \tag{18}$$

where the property of derivation of Kummer functions (see (13.4.8) of [20])

$$\frac{\partial \mathscr{K}(a,b,z)}{\partial z} = \mathscr{K}'(a,b,z) = \frac{a}{b}\,\mathscr{K}(a+1, b+1, z)$$

has been used. Eq. (18) does not allow any analytical solution for Γ. Numerical calculations will be derived in the next section. Before giving these results, we study the compatibility of this dispersion equation (18) with the no flow configuration.

4.2. Compatibility of solution with the no flow configuration

Using the Taylor development of Kummer functions (see (13.1.2) of [20])

$$\mathscr{K}(a,b,z) = \sum_{n=0}^{\infty} \frac{(a)_n z^n}{(b)_n n!}$$

and the following definition and properties of the Pochhammer coefficient $(x)_n$:

$$(x)_n = x(x+1)\ldots(x+n-1) = \frac{\Gamma(x+n)}{\Gamma(x)} = \prod_{i=0}^{n-1}(x+i) \quad \text{and} \quad (x)_0 = 1,$$

$$(x+1)_n = \frac{(x)_n \times (x+n)}{x} \quad \text{and} \quad (x)_n \times \alpha^n = \prod_{i=0}^{n-1}[\alpha(x+i)]$$

allows us to develop Eq. (18) in the Taylor series

$$\sum_{n=0}^{\infty} \frac{(A)_n}{(m+1)_n}\left(\frac{\alpha}{2}\right)^n \frac{1}{n!}\left(\frac{2m+a-\alpha}{2} + \frac{(A+n)\alpha}{m+n+1}\right) = 0.$$

If $\mathscr{M} \longrightarrow 0$ this series reduces to

$$(m!)\sum_{n=0}^{\infty} \frac{(-1)^n b^n}{4^n (m+n)! n!}\left(m - \frac{b}{2(m+n+1)}\right) = 0,$$

which is a development of Bessel functions of the first kind (see (9.1.10) of Ref. [20]). Indeed, this equation can also be written as (making use of Bessel functions properties (9.1.27) of Ref. [20])

$$\frac{2^m m!}{(\sqrt{b})^{m-1}}\left(\frac{m}{\sqrt{b}}J_m\left(\sqrt{b}\right) - J_{m+1}\left(\sqrt{b}\right)\right) = \frac{2^m m!}{(\sqrt{b})^{m-1}}J'_m\left(\sqrt{b}\right) = 0.$$

These solutions are exactly those found without flow (zeros of the derivative of Bessel functions of the first kind). This shows that the dispersion equation (18) converges to the well known no flow one when the Mach number tends towards zero.

5. Effect of laminar shear flow

In this section, the effect of laminar shear flow on the cut-off frequency, propagation constant and pressure profiles is discussed. Then, dispersion curves are plotted in an attempt to isolate effects of refraction. Whenever possible, results are compared with the literature to validate the proposed analytical solution.

5.1. Cut-off frequency

After the expression of the dispersion equation has been established, the analysis of the evolution of cut-off frequencies against the Mach number is generally studied. Among others, Agarwal and Bull [12] showed that turbulent shear flow makes cut-off frequencies of each mode decrease with an increasing Mach number, in downstream configuration. They found that cut-off frequencies for laminar subsonic flow shift less than turbulent ones but still shift slightly compared with the no flow ones. This has been confirmed by Pagneux and Froelich [10].

Cut-off frequencies are found from the dispersion equation (Eq. (18) in the case under study) by imposing a propagation constant (Γ) equal to zero. This operation leads to

$$\frac{2^m m!}{\left(\sqrt{b}\right)^{m-1}}\left(\frac{m}{\sqrt{b}}J_m\left(\sqrt{b}\right)-J_{m+1}\left(\sqrt{b}\right)\right)=\frac{2^m m!}{\left(\sqrt{b}\right)^{m-1}}J'_m\left(\sqrt{b}\right)=0.$$

This equation shows that the zeros found are also those of no flow configuration. In others words, cut-off frequencies in laminar subsonic flow are found to be the same as no flow ones. This contradiction with previous results [10,12] can be explained by the fact that the coefficients of the differential equation (10) have been approximated at first order to get a solvable equation. Therefore our development is not able to handle a calculation of the cut-off frequencies accurate enough to obtain the expected shift in frequencies. Accordingly, Pagneux and Froelich [10] showed that the deviation of cut-off frequencies increases with $|\Gamma\mathscr{M}|^2$. This term is of order two and we restrict ourselves to the first order when approximating the differential equation. This explains why we cannot describe the shift in cut-off frequencies induced by laminar shear flow.

Nevertheless, our model allows us to calculate the propagation constant, to derive pressure profiles and dispersion curves and to compare our results with the ones available in the literature. This is done in the following.

5.2. Propagation constant

In order to obtain the propagation constant in the presence of a laminar shear flow, the function $F(\Gamma)$ (Eq. (18)) is plotted numerically for a set of parameters Ω, $\mathscr{M}$ and m, that is for a given working frequency, Mach number and circumferential order. Approximated values of roots $\Gamma_{m,n}$ are given by zeros of the function F. In order to facilitate comparison of the present results with previous works, the Mach number has been transformed into a Mach number associated with volume flow according to

$$\mathscr{M}_v=\frac{1}{S}\int_S\mathscr{M}(\xi)\,\mathrm{d}s=C\mathscr{M}_0, \tag{19}$$

where S is the section area and C is a coefficient which, in the case of laminar shear flow in a circular duct, is equal to $\frac{1}{2}$.

Table 1
Downstream wavenumber Γ_d for propagative modes against $\mathscr{M}_v$, for $\Omega=1$ and 3.5 in the case of laminar shear flow and uniform flow

Γ_d	$\Omega=1$		$\Omega=3.5$					
$\mathscr{M}_v$	$\Gamma_{0,0}$	$\Gamma_{0,0}^{\text{unif.flow}}$	$\Gamma_{0,0}$	$\Gamma_{0,0}^{\text{unif.flow}}$	$\Gamma_{1,0}$	$\Gamma_{1,0}^{\text{unif.flow}}$	$\Gamma_{2,0}$	$\Gamma_{2,0}^{\text{unif.flow}}$
0	1.0000	1.0000	1.0000	1.0000	0.8505	0.8505	0.4884	0.4884
0.01	0.9899	0.9901	0.9900	0.9901	0.8413	0.8406	0.4794	0.4785
0.05	0.9498	0.9524	0.9508	0.9524	0.8055	0.8029	0.4451	0.4414
0.10	0.8999	0.9091	0.9036	0.9091	0.7622	0.7597	0.4056	0.4001
0.15	0.8511	0.8696	0.8583	0.8696	0.7207	0.7203	0.3699	0.3638
0.20	0.8039	0.8333	0.8151	0.8333	0.6813	0.6843	0.3379	0.3319
0.25	0.7589	0.8000	0.7742	0.8000	0.6441	0.6513	0.3094	0.3039
0.30	0.7163	0.7692	0.7354	0.7692	0.6092	0.6208	0.2841	0.2792

Some results of this computation are reported in Table 1 in the case of downstream propagation for $\Omega = 1$ and 3.5 and for different Mach numbers. In this table, for a given working frequency, the values of Γ for the (m,n) mode, noted $\Gamma_{m,n}$, are given in the column on the left, while values of Γ for uniform flow configuration, noted $\Gamma_{m,n}^{\text{unif.flow}}$, are reported in the column on the right. As shown by the comparison between the second and fourth columns of Table 1 ($\Gamma_{0,0}^{\text{unif.flow}}$ for $\Omega = 1$ and for $\Omega = 3.5$ as a function of the Mach number), and as expected [1], the propagation constant $\Gamma_{0,0}^{\text{unif.flow}}$ is independent of frequency and depends on the Mach number according to

$$\Gamma_{0,0}^{\text{unif.flow}} \sim \frac{1}{1 \pm \mathscr{M}}. \tag{20}$$

Then, comparing the first and third columns of Table 1, which give $\Gamma_{0,0}$ for laminar subsonic flow for $\Omega = 1$ and 3.5, it appears, in agreement with Agarwal and Bull [12], that shear flow makes Γ frequency dependent, that is shear flow makes the plane mode dispersive.

Values of Γ in the upstream configuration were also computed and results are reported in Table 2. This table shows that in this configuration, for a given mode (i.e. a given column), Γ increases when the Mach number increases as expected. It also appears that when the non-dimensional frequency Ω increases, Γ increases, as found by Pagneux and Froelich [10].

Deviation of the propagation constant is due to both convective effect, which is responsible for deviation of uniform flow constants, and to refractional effect, responsible for the difference between uniform flow and laminar shear flow configurations.

The calculation of the propagation constant allows us to obtain pressure profiles (Eq. (13)) for a given Mach number and working frequency Ω. Results of such a calculation are presented in the next section.

Table 2
Upstream wavenumber Γ_u for propagative modes against $\mathscr{M}_v$, for $\Omega = 1$ and 3.5 in the case of laminar shear flow and uniform flow

Γ_u	$\Omega = 1$		$\Omega = 3.5$					
$\mathscr{M}_v$	$\Gamma_{0,0}$	$\Gamma_{0,0}^{\text{unif.flow}}$	$\Gamma_{0,0}$	$\Gamma_{0,0}^{\text{unif.flow}}$	$\Gamma_{1,0}$	$\Gamma_{1,0}^{\text{unif.flow}}$	$\Gamma_{2,0}$	$\Gamma_{2,0}^{\text{unif.flow}}$
0	1.0000	1.0000	1.0000	1.0000	0.8505	0.8505	0.4884	0.4884
0.01	1.0099	1.0101	1.0100	1.0101	0.8595	0.8605	0.4974	0.4985
0.05	1.0495	1.0526	1.0508	1.0526	0.8966	0.9031	0.5349	0.5417
0.10	1.0974	1.1111	1.1032	1.1111	0.9436	0.9617	0.5844	0.6021
0.15	1.1429	1.1765	1.1573	1.1765	0.9912	1.0272	0.6361	0.6707
0.20	1.1851	1.2500	1.2130	1.2500	1.0387	1.1010	0.6893	0.7486
0.25	1.2234	1.3333	1.2707	1.3333	1.0859	1.1846	0.7431	0.8372
0.30	1.2575	1.4286	1.3310	1.4286	1.1323	1.2802	0.7967	0.9386

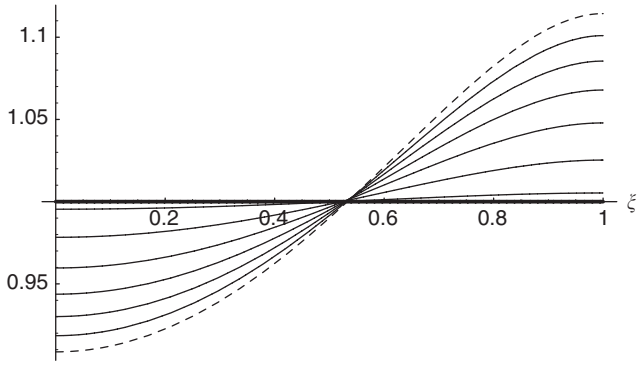

Fig. 3. Profiles of mode (0,0) for $\Omega = 2$ against Mach number (0–0.3)—downstream configuration.

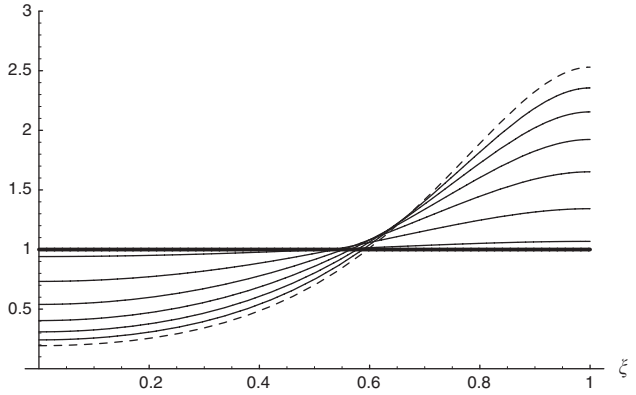

Fig. 4. Profiles of mode (0,0) for $\Omega = 7.25$ against Mach number (0–0.3)—downstream configuration.

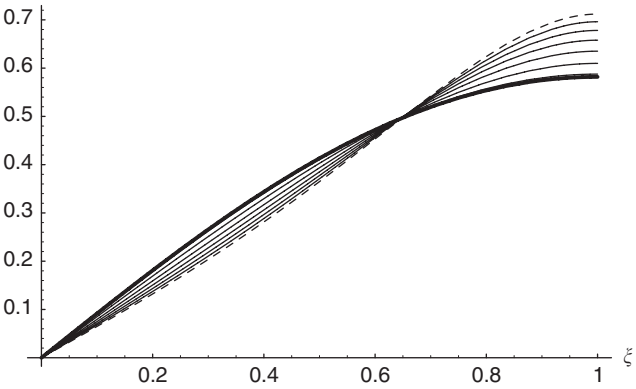

Fig. 5. Profiles of mode (1,0) for $\Omega = 4$ against Mach number (0–0.3)—downstream configuration.

5.3. Pressure profiles

As stated above, deviation of the propagation constant is due to both convection and refraction. On the other hand, deviation of the pressure profile is due only to refraction. Figs. 3 and 4 present the acoustic pressure profiles of mode (0,0) at a non-dimensional frequency $\Omega = 2$ and 7.25, respectively, for different Mach numbers (0–0.01–0.05–0.1–0.15–0.2–0.25–0.3). The no flow solution is represented by a bold curve. The curve corresponding to the higher Mach number ($\mathscr{M} = 0.3$) is represented by a dashed line. The profiles have been normalized with respect to the no flow profile integrated over the section. These figures clearly show that, as expected (e.g. Ref. [21]), the deformation increases with an increasing Mach number. Comparison between Figs. 3 and 4 which correspond to the same configuration but different working frequencies shows that, as expected (e.g. Ref. [10]), the higher the frequency, the more deformed the pressure profile. Further calculations show that in the upstream configuration, pressure profiles of the plane mode are also more deformed when the Mach number and/or the frequency increases.

As expected (e.g. Ref. [13]), in downstream propagation (respectively, upstream propagation), profiles present a re-distribution of pressure towards the wall (respectively towards the core). This effect is due to mean velocity gradients which, in downstream (respectively, upstream) configuration refract acoustic waves towards the wall (respectively, towards the core). Similar tendencies are found for higher modes. For example, comparison between Figs. 5 and 6 which correspond to the mode (1,0), i.e. the first circumferential mode, at working frequencies $\Omega = 4$ and 10 shows that the deformation of the pressure profile increases when the Mach

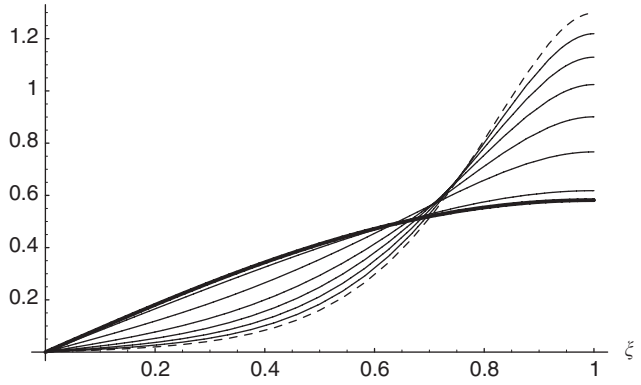

Fig. 6. Profiles of mode (1,0) for $\Omega = 10$ against Mach number (0–0.3)—downstream configuration.

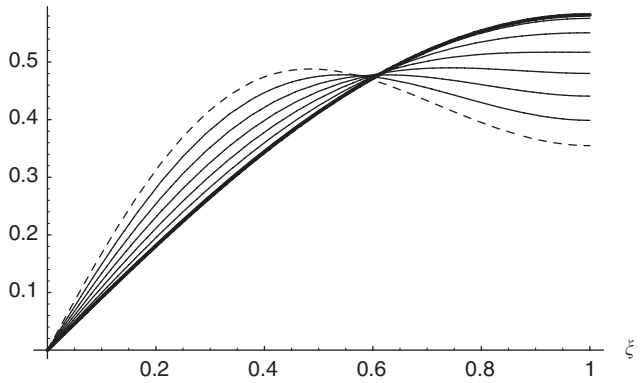

Fig. 7. Profiles of mode (1,0) for $\Omega = 4$ against Mach number (0–0.3)—upstream configuration.

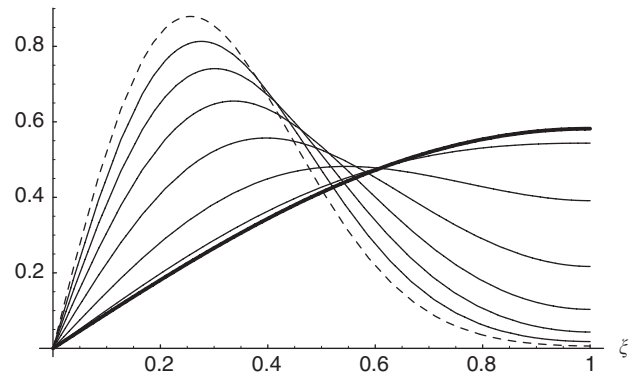

Fig. 8. Profiles of mode (1,0) for $\Omega = 10$ against Mach number (0–0.3)—upstream configuration.

number and the frequency increase. These results are in agreement with those of Pagneux and Froelich [10], Bihhadi and Gervais [13,14] and Yehya [21].

Figs. 7 and 8 present the evolution of profiles of mode $(1, 0)$ in the same configuration as Figs. 5 and 6 except that the wave is upstream propagating. As expected [13,14,21], the acoustic pressure increases at the core whereas it decreases near the wall, as in downstream propagation; profiles are also more deformed when the working frequency increases.

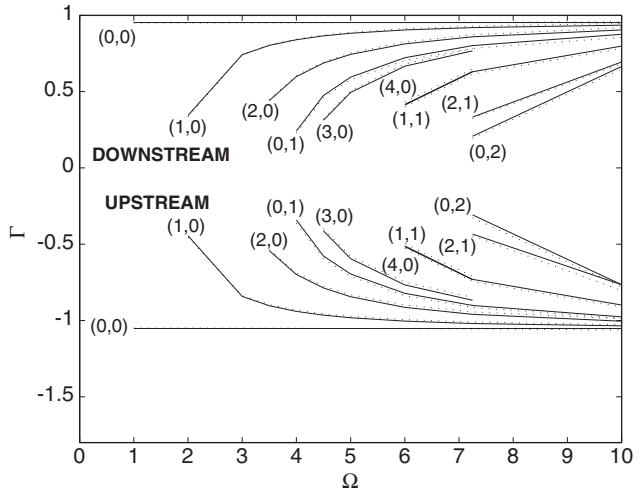

Fig. 9. Dispersion curves ($\Gamma = F(\Omega)$) for both downstream and upstream propagation, for all propagative modes (m, n) at $\mathscr{M}_v = 0.05$. Solid line: uniform flow configuration, dotted line: laminar one.

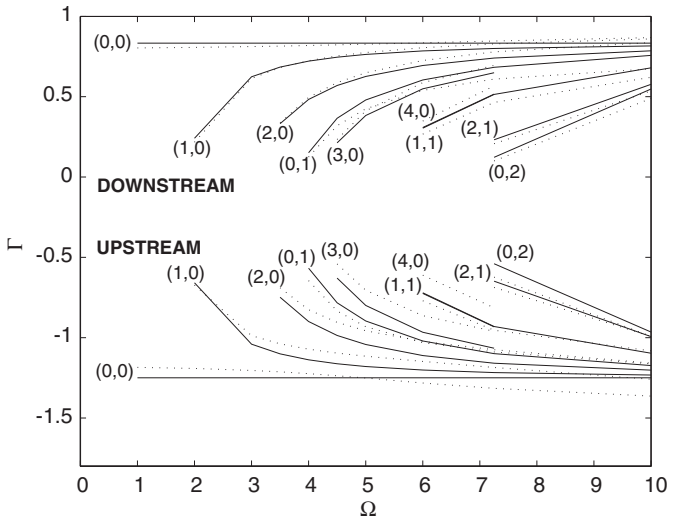

Fig. 10. Dispersion curves ($\Gamma = F(\Omega)$) for both downstream and upstream propagation, for all propagative modes (m, n) at $\mathscr{M}_v = 0.2$. Solid line: uniform flow configuration, dotted line: laminar one.

The refractional effect increases with frequency and with gradient, which is why profiles are more deformed if the Mach number or working frequency increases.

Results obtained so far on this matter are in agreement with previous numerical results and this validates our analytical solution.

In order to appreciate further the effect of shear flow, dispersion curves are presented in the next section.

5.4. Dispersion curves

Dispersion curves, which are propagation constant versus frequency, have also been plotted. Fig. 9 shows the dispersion curves at Mach number 0.05 for several modes (m, n) while Fig. 10 shows the dispersion curves at Mach number 0.2. Upstream values of the propagation constant were set into the negative on these figures for ease of comparison of downstream and upstream configurations. Results shown in Fig. 10 are in

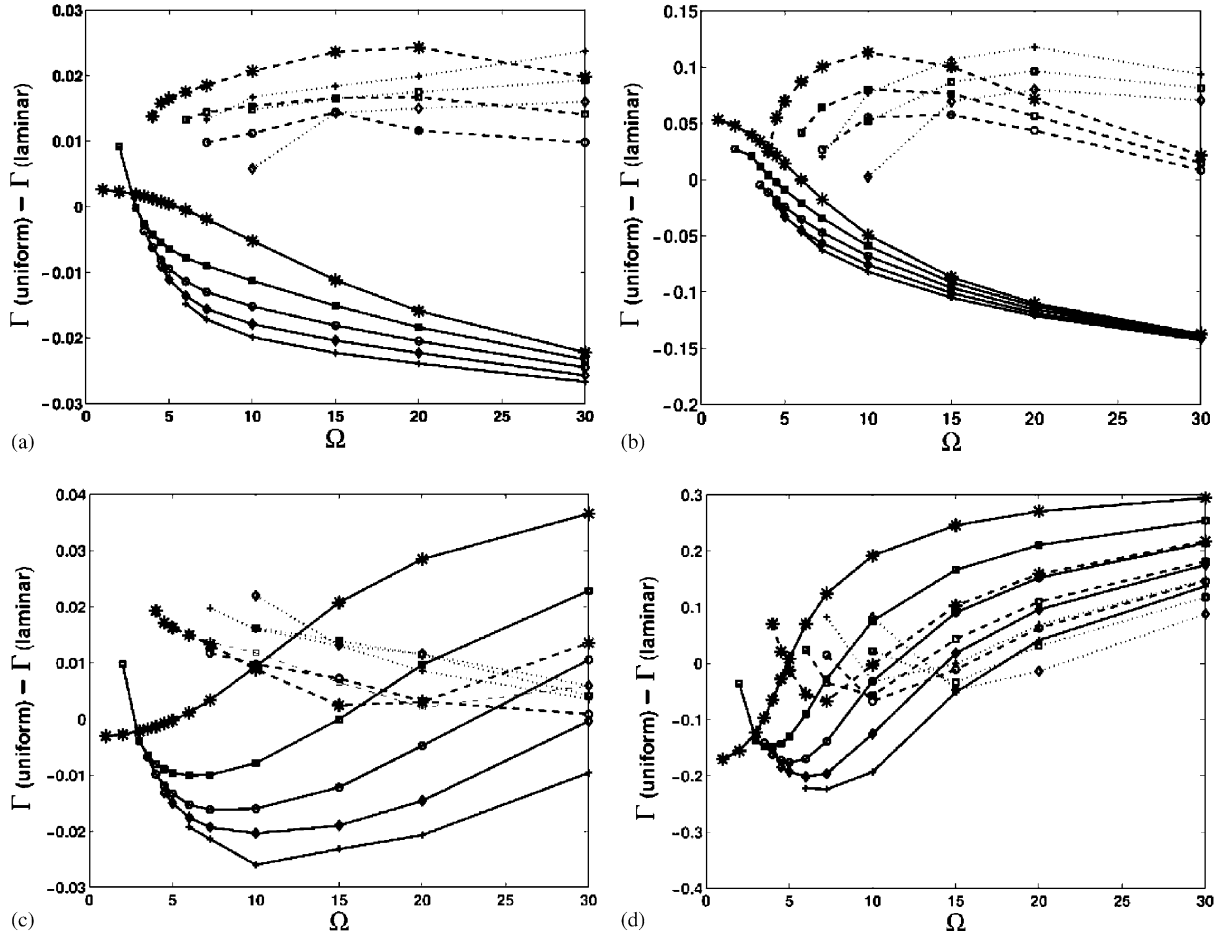

Fig. 11. Difference of propagation constant for different configuration: –✱: mode (0,0), –□: mode (1,0), —○: mode (2,0), —◇: mode (3,0), —+: mode (4,0), - -✱: mode (0,1), - -□: mode (1,1), - -○: mode (2,1), ...+: mode (0,2), ...□: mode (1,2), . . .◇: mode (2,2). (a) Downstream—Mach = 0.05; (b) downstream—Mach = 0.3; (c) upstream—Mach = 0.05; (d) upstream—Mach = 0.3.

agreement with numerical computations conducted by Bihhadi and Gervais [13]. Small discrepancies between our results and theirs can be attributed to the fact that they studied the case of a rectangular duct. The difference between the uniform and shear flow propagation constant is more important at Mach number 0.2 than 0.05, which confirms that shear flow effect increases with an increasing Mach number. Deviation of the propagation constant from the uniform case is more pronounced in the upstream configuration than in the downstream one, in agreement with previously presented results. It may also be noted that, comparing Figs. 9 and 10, all curves are shifted towards lower values. As noted by Bihhadi and Gervais [13], this is due to convection.

As stated above, deviation of the propagation constant from the no flow case is due to both convection and refraction, whereas deformation of the profile is due only to refraction. Therefore, in order to compare the effects of shear flow with uniform flow, differences between uniform flow propagation constants and laminar ones have been calculated for several configurations. These differences have been plotted in Figs. 11(a) and (b) for downstream configuration at Mach numbers 0.05 and 0.3, respectively. In this configuration, distinct behaviours are noticeable, depending on the radial order of the mode (n), that is curves corresponding to similar values of n form a given set. For all modes (m,0), that is for all non-radial modes (purely circumferential modes), represented by solid lines, curves decrease when Ω increases for both $\mathscr{M} = 0.05$ and 0.3. All these curves seem to converge at high Ω towards the same asymptote. On the other hand, curves of first-order radial modes (m,1), represented by dashed lines, present a bump as Ω increases before converging at

high Ω. For second-order radial modes (m,2), represented by dotted lines, curves also present a bump but seem to shift towards higher frequencies compared with first radial order modes. They also seem to converge for high working frequency.

Figs. 11(c) and (d) present the evolution of $\Gamma_{\text{uniform}} - \Gamma_{\text{laminar}}$ in upstream configuration at Mach numbers 0.05 and 0.3, respectively. Although tendencies appear less clearly than in downstream configuration, one can still distinguish a set of curves corresponding to similar radial mode order. In any case, the difference between the uniform and laminar propagation constant in upstream configuration first present a tough as frequency increases and then seem to converge towards the same asymptote.

There are no similar results in the literature for comparison with the present ones as previous works did not consider the evolution of the propagation constant for non-axi-symmetric modes. Even if the physical reason of such behaviour is left unexplained, our study shows that the effect of shear flow depends on the radial order of the propagating mode.

6. Conclusion

An analytical solution of the wave equation in circular ducts in the presence of laminar shear flow was derived. Connections between this solution and already-known solutions of more specific cases were made. In order to validate the proposed analytical solution and to study the effect of shear flow on multimodal propagation, the propagation constant was calculated. It was found that the latter decreases (respectively, increases) with the Mach number in the case of downstream (respectively, upstream) propagation, as a result of convection. Propagation constants were found to be frequency dependent due to shear in the flow. It appeared that the effect of shear flow is associated with the deformation of profiles which depends on Mach number and frequency. It was found that pressure profiles shift more and are more deformed in the upstream configuration than in the downstream one. In downstream configuration (respectively, upstream), profiles present a redistribution of pressure towards the wall (respectively, toward the core). All these results are in agreement with previous findings and consolidate our analytical solution proposed. Our study also showed that the effect of shear flow is strongly linked to the radial order of the propagating mode. Further studies should be concerned with experimental confirmation of this tendency which hopefully will make physical interpretation easier.

Acknowledgements

Authors are indebted to Professor Gervais for fruitful discussion and advice.

Appendix

Kummer function: The confluent hypergeometric Kummer functions $\mathscr{K}(a,b,z)$ are the ensemble of solutions of the differential equation

$$z\frac{\partial^2 f}{\partial z^2} + (b-z)\frac{\partial f}{\partial z} - af = 0.$$

Like Bessel equation admits for solutions Bessel functions of first kind J_n and Bessel function of second kind Y_n, Kummer equation admits Kummer's M-function (regular at $z=0$), and Kummer's U-function (singular at $z=0$). Kummer functions form part of confluent hypergeometric function as Whittaker functions.

Defining $\alpha = \sqrt{a^2 - 4c}$, it can be proved that the function

$$\mathrm{e}^{(a-\alpha)\xi^2/4}\xi^m \mathscr{K}\left(\frac{(m+1)\alpha - (a+b)}{2\alpha}, m+1, \frac{\alpha}{2}\,\xi^2\right)$$

is the solution of the differential equation

$$\frac{\partial^2 f}{\partial \xi^2} + \left(\frac{1-a\xi^2}{\xi}\right)\frac{\partial f}{\partial \xi} + \left(b + c\xi^2 - \frac{m^2}{\xi^2}\right)f = 0.$$

References

[1] M. Bruneau, *Manuel d'Acoustique Fondamentale*, Hermes, Paris, 1998.
[2] A. Hirschberg, S.W. Rienstra, *An Introduction to Acoustics*, Eindhoven University of Technology, 1992.
[3] P.N. Shankar, Sound propagation in duct shear layers, *Journal of Sound and Vibration* 22 (2) (1972) 221–232.
[4] S.D. Savkar, Propagation of sound in ducts with shear flow, *Journal of Sound and Vibration* 19 (3) (1971) 355–372.
[5] E. Perrey-Debain, Y. Gervais, M. Guilbaud, Extension de la DRBEM à la propagation guidée en écoulement cisaillé, *Comptes Rendus de l Academie des Sciences* 326 (IIb) (2000) 429–436.
[6] D.C. Pridmore-Brown, Sound propagation in a fluid through an attenuating duct, *Journal of Fluid Mechanics* 4 (1958) 393–406.
[7] P. Mungur, H.E. Plumbee, Propagation and attenuation of sound in a soft walled annular duct containing shear flow, NASA SP-207, 1969, pp. 305–322.
[8] G.R. Gogate, M.L. Munjal, Analytical solution of sound propagation in lined or unlined circular ducts with laminar mean flow, *Journal of Sound and Vibration* 160 (3) (1993) 465–484.
[9] G.R. Gogate, M.L. Munjal, Sound propagation in ducts with bulk reacting lining in the presence of laminar mean flow, *Journal of the Acoustical Society of America* 99 (3) (1996) 1779–1782.
[10] V. Pagneux, B. Froelich, Influence of low Mach number shear flow on acoustic propagation in ducts, *Journal of Sound and Vibration* 246 (1) (2001) 137–155.
[11] J.L. Peube, M.F. Jallet, Propagation d'ondes acoustiques dans un écoulement en conduite cylindrique, *Acustica* 29 (1973) 86–92.
[12] N.K. Agarwal, M.K. Bull, Acoustic wave propagation in a pipe with fully developed turbulent flow, *Journal of Sound and Vibration* 132 (2) (1989) 275–298.
[13] A. Bihhadi, Y. Gervais, A finite difference method for acoustic wave propagation in a duct with mean flow and temperature gradients, *Acta Acustica* 2 (1994) 343–357.
[14] A. Bihhadi, Y. Gervais, Analysis of the distribution and attenuation of acoustic energy flow in lined duct containing inhomogeneous medium by the finite difference method, *Acustica—Acta Acustica* 83 (1997) 1–12.
[15] B. Karthik, R.K. Mohanraj, R. Ramakrishnan, R.I. Sujith, Exact solution for sound propagation in ducts with an axial mean temperature gradient and particulate damping, *Journal of the Acoustical Society of America* 106 (5) (1999) 2391–2395.
[16] B. Karthik, B.M. Kumar, R.I. Sujith, Exact solutions to one-dimensional acoustic fields with temperature gradient and mean flow, *Journal of the Acoustical Society of America* 108 (1) (2000) 38–43.
[17] S.H. Ko, Theoretical prediction of sound attenuation in acoustically lined annular ducts in presence of uniform flow and shear flow, *Journal of the Acoustical Society of America* 54 (6) (1973) 1592–1606.
[18] S.K. Kakoty, V.K. Roy, Bulk reaction modeling of ducts with and without flow, *Journal of the Acoustical Society of America* 112 (1) (2002) 75–83.
[19] M.K. Bull, N.K. Agarwal, Propagation of acoustic waves in fully-developed turbulent pipe flow, 11e ICA, Paris, 1983, pp. 295–298.
[20] M. Abramowitz, I.A. Stegun, *Handbook of Mathematical Functions*, National Bureau of Standards, New York, 1964.
[21] Y. Yehya, Propagation des Ondes Acoustiques dans les Conduites Cylindriques de Révolution, Thèse de Doctorate, Université de Poitiers, 1988.